Release Kinetics Studies of Aromatic Molecules into Water from Block Polymer Micelles

Yue Teng, M. E. Morrison,† P. Munk,* and S. E. Webber*

Department of Chemistry and Biochemistry and the Center for Polymer Research, The University of Texas at Austin, Austin, Texas 78712

Karel Procházka*

Department of Physical and Macromolecular Chemistry, Charles University in Prague, Albertov 2030, 12840 Prague 2, Czech Republic

Received November 24, 1997; Revised Manuscript Received April 9, 1998

ABSTRACT: Micelles formed from amphiphilic block copolymers are known to effect aqueous solubilization of hydrophobic molecules. The kinetics of uptake or release can be monitored by fluorescence if the solubilizate is a fluorophore. The primary objective of this paper is the characterization of the release kinetics in aqueous solution of two hydrophobic fluorescent probes (pyrene and phenanthrene) loaded into polymer micelles composed of the following diblock polymers: polystyrene-*block*-poly(methacrylic acid), poly(*tert*-butyl acrylate)-*block*-poly(2-vinylpyridine), poly(2-vinylpyridine)-*block*-poly(ethylene oxide). Polystyrene latex particles were also studied for comparison. The release process was analyzed by a model of diffusion out of a sphere and the diffusion constants we measure are very small (10^{-18}−10^{-16} cm^2/s), depending on the core and probe. An exception is poly(2-vinylpyridine) for which the release was too fast for our measurement technique. Independent measurements of the partition coefficient of the probes between the micelle and water demonstrated that the micelles are very effective at solubilization (partition coefficients from 3×10^4 to 3×10^5 were obtained, depending on the micelle−probe combination). Consideration of the partition coefficient, fluorescence quenching of the solubilized probe by Tl^+, and the release kinetics has suggested a "three-region" model for solubilization of hydrophobic molecules in this class of polymer micelles: (1) The first is the core, which for several of our systems is glassy. Diffusion from a glassy core is very slow. (2) The second is an "inner corona", composed of the hydrophilic block polymer which may be swollen by water but its ionization, by gain or loss of protons, is suppressed. The important role of the inner corona in solubilization was not appreciated by us in our earlier study of phenanthrene released from two different PS−PMA micelles. In some cases the majority of the solubilized probe appears to be located in this region. (3) Finally, there is an "outer corona" for which the chains are not crowded and which may sustain a significant charge density. Probe molecules solubilized in this region are accessible to the Tl^+ quencher.

Introduction

Copolymers containing blocks of different solvent selectivity can self-assemble into spherical micelle structures in which the poorly solvated block forms the micelle core and the well-solvated block forms the micelle corona (or shell). Micelles formed from many block- and graft-copolymers in organic media have been systematically studied and reviewed.[1] A smaller number of copolymers which form micelles in aqueous solutions have been studied. Aqueous polymer micelles are of special interest due to their ability to enhance the solubility of hydrophobic molecules in aqueous solutions.[2] Such properties are potentially significant in technologies including drug delivery[3] and environmental cleanup.[2e]

We have carried out a number of studies of aqueous phase micelles formed from polystyrene-*block*-poly(methacrylic acid) (PS−PMA).[4] The hydrophobic polystyrene block forms the micelle core while the poly(methacrylic acid) block forms the micelle corona. The PS−PMA micelle has excellent stability over a broad range of concentrations, ionic strengths, and pH. The glassy polystyrene core ($T_g = 373$ K and not swollen by water) appears to help anchor the stretched poly(methacrylic acid) chains of the corona and keep the micelle from dissociating into its unimer components. More recently we have also studied polymers with poly(2-vinylpyridine) cores[5] or coronas (depending on the state of protonation of the pyridine) and produced a multilayer "onion" micelle with a poly(*tert*-butyl acrylate) "inner core", poly(2-vinylpyridine) "outer core", and PEO corona.[6]

In addition to structural investigations, we have studied the solubilization of hydrophobic molecules by PS−PMA in aqueous solutions. Motivated by the potential application of this type of micelle as a vehicle for hydrophobic drug delivery, a study was published on the release kinetics of phenanthrene from the PS−PMA micelle.[7] The present paper builds on this previous work and describes studies of the release kinetics of the polycyclic aromatic hydrocarbons pyrene and phenanthrene from several classes of diblock polymer micelles. Following our earlier approach, fluorescence methods are used to monitor the release process and our analysis of the data is based on simple diffusion from a sphere into a reservoir.[7] The solution to Fick's law for this case depends on the parameter D/r_{core}^2, where D is the diffusion constant and r_{core} is the radius of the spherical core. The fit of the experimental data to the theoretical model permits an evaluation of the diffusion coefficient of the fluorescence probes if r_{core} can

† Current address: IBM Almaden Research Center, 650 Harry Rd., San Jose, CA 95120-6099.

S0024-9297(97)01721-X CCC: $15.00
Published on Web 05/15/1998

Table 1. Distribution Coefficients and Solubilization for Various Polymer Micelles

sample (mg/mL)[e]	probe	K_D^0 [a]	x_{buffer}^0 [b]	K_P^0 [c]	concn (μM)[d]
PS−PMA (3.5)	pyrene	656	0.0015	1.87×10^5	369 ± 4
PS−PMA (3.5)	Phen	331	0.0030	0.946×10^5	1310 ± 14
PS latex (1.86)	pyrene	573	0.0017	3.09×10^5	324 ± 3
PS latex (2.15)	Phen	218	0.0046	1.01×10^5	843 ± 11
PBA−PVPH$^+$ (3.2)	pyrene	366	0.0027	1.14×10^5	206 ± 4
PBA−PVPH$^+$ (3.6)	Phen	154	0.0065	4.28×10^4	589
PVP−PEO (1.8)	pyrene	55.6	0.0177	3.09×10^4	26.6
PBA−PVP/PVP−PEO (0.93)	pyrene	87.8	0.0112	9.44×10^4	48.3 ± 0.3
PBA−PVP/PVP−PEO (0.93)	Phen	37.9	0.0257	4.08×10^4	118 ± 2
water	pyrene				0.41(±0.16)
	Phen				4.75(±0.08)

[a] Determined by fluorescence method, see eq 1 of text. [b] $x_{buffer}^0 = (1 + K_D^0)^{-1}$, the fraction of probe in the aqueous buffer phase. [c] See eq 2 of text. [d] Concentration of probe in micelle solution, including the contribution from the bulk buffer solution, based on the fluorescence method calibration curve. [e] Concentration of micelle (or latex).

be estimated. The release kinetics from micelles are compared with those from polystyrene latexes, which one might consider as a model system for the PS−PMA micelle core. In our prior work the role of the corona was ignored in the solubilization and release kinetics of the probe. The studies reported here demonstrate that the corona plays an important role in solubilization. By combining measurements of the distribution coefficient and the fluorescence quenching of solubilized probes with the release kinetics, we believe a much more complete picture has emerged. We should add that alternative photophysical methods based on time-dependent fluorescence and nonradiative energy transfer can be used to assess the partitioning and rate of transfer of hydrophobic probes between polymer micelles.[4h,8] Fluorescence methods have also been used to assess the rate of polymer exchange between micelles.[9−12]

The use of fluorescence probes to characterize surfactant micelles is well-established.[13] The physical situation for these studies is quite different from the present case because the surfactant molecules are rapidly exchanged with the bulk and as a consequence the probe molecules are also rapidly exchanged. The physical dimensions of a surfactant micelle are at least an order of magnitude smaller than those for polymer micelles, such that application of the classical diffusion model that we use in our analysis is dubious. Winnik and co-workers have used phosphorescence quenching of 4-bromo-1-acetonaphthone (BAN) by $NaNO_2$ to estimate the exit and entry rates of BAN into polystyrene-*b*-poly(ethylene oxide) micelles.[14] This experiment was analyzed in the same theoretical framework used for surfactant micelles. The triplet state of BAN has a lifetime of ca. 400 μs, such that exit and entry can occur during the lifetime of ^{3}BAN*. The solubility of BAN in water is quoted as 1.1×10^{-4} M, approximately 25 times larger than our most soluble probe, phenanthrene (see Table 1). As a consequence relatively little of the BAN resides within the micelle and no relation of the exit rate to the micelle core size is found. Winnik et al. conclude that the solubilized BAN probe resides near the core−surface interface, which is consistent with our solubilization model discussed later.

Experimental Section

Polymer Samples. The synthesis and characterization of the PS−PMA copolymer was reported elsewhere.[15] The weight fraction of the PS block (W_{PS}) is 0.64, as determined by NMR analysis. The weight-averaged molecular weights of the PS and PMA blocks are 2.83×10^4 and 1.54×10^4, respectively, as determined by GPC and NMR analyses. The molecular weight of the PS−PMA micelle is 1.25×10^7 (corresponding to an aggregation number of 286), based on static light scattering measurements by Dr. Zdenek Tuzar.[16] Suspensions of monodisperse polystyrene latexes (64 nm diameter) were used as received from Polysciences, Inc. 1,4-Dioxane was used as received from EM Science. Deionized water and dioxane were used in the dialysis procedure for the preparation and loading of the PS−PMA copolymer micelle and latex samples.

The synthesis and characterization of the poly(*tert*-butyl acrylate)-*block*-poly(2-vinylpyridine), PBA−PVP, was described elsewhere.[6a] The poly(vinylpyridine) block (PVP) has a molecular weight (M_w) of 2.7×10^4, $M_w/M_n = 1.07$, and a weight fraction of 0.47 in the final copolymer. For the copolymer, $M_w = 7.9 \times 10^4$ and $M_w/M_n = 1.27$. The molecular weight of the PBA−PVPH$^+$ micelle was 1.46×10^7 g/mol measured by static light scattering measurements. Most pyridines are protonated under the pH = 1 conditions used to prepare the micelles). The poly(2-vinylpyridine)-*block*-poly(ethylene oxide) copolymer, PVP−PEO, was obtained from Polymer Source, Inc., Quebec, Canada. For the PVP block $M_w = 1.4 \times 10^4$ and $M_w/M_n = 1.03$, with a weight fraction of 0.48 in the copolymer. For the copolymer $M_w = 2.9 \times 10^4$ and $M_w/M_n = 1.05$. The solvents 1,4-dioxane, methanol, and 0.1 M HNO_3 were used in the dialysis procedure for the preparation and loading of the PBA−PVPH$^+$ copolymer micelles. A 0.01 M HCl solution was used as the dilution medium for the release from the PBA−PVPH$^+$ micelle sample,[17] and a pH 7 phosphate buffer was used for PVP−PEO or onion type micelles.

Micelle Preparation and Loading with Probe. A 5.0 mg/mL PS−PMA copolymer micelle solution was prepared by dissolving PS−PMA directly into a dioxane/water mixture with a dioxane volume fraction (V_D) of 0.8.[4c] The micelle solution was then dialyzed stepwise against dioxane/water mixtures with V_D values of 0.6, 0.4, 0.2, 0.1, and 0. The dialysis at each step was against a 50-fold volume excess for a minimum of 3 h. For the preparation of loaded micelle solutions the dialysis was against a saturated chromophore solution at the $V_D = 0.2$ dialysis step for at least 12 h. In the subsequent dialysis steps, the micelles were dialyzed against chromophore-saturated solutions in order to maintain saturation of chromophore in the micelle. The loaded micelle solution was then filtered (0.45 μm pore size, Aerodisk LC13 PVDF) and left to stand several days prior to the release measurements to allow for an equilibrium distribution of the probe. We use dioxane/water mixtures in the loading procedure in order to plasticize the micelle core which helps ensure that the core is homogeneously loaded.

The latex samples were prepared by a 10-fold dilution of the original 2.67% solids suspension. The loading procedure involved the 10-fold dilution of the original suspension into a chromophore saturated dioxane/water mixture with $V_D = 0.2$. After being stirred for a minimum of 12 h, the solution was dialyzed against chromophore-saturated water. After dialysis, the loaded-latex solution was filtered and left to stand several days prior to the release studies.

A 10 mg/mL PBA−PVP copolymer micelle solution was prepared by dissolving PBA−PVP sample directly into a 1,4-dioxane/methanol (70/30 V/V). After dissolution, methanol was slowly added to 50 vol % content and then the 0.1 M HNO_3 solution was added dropwise to 50% of the resulting total volume. Both of the steps were carried out with vigorous stirring. The micelle solution was then dialyzed against 0.1 M HNO_3. Because the vinylpyridine is largely protonated, we refer to this micelle as PBA−PVPH$^+$. For the preparation of loaded micelle solutions, the hydrophobic probes were added from the beginning. The loaded PBA−PVPH$^+$ micelles were

mixed with PVP−PEO copolymers (weight ratio 1/1) which was molecularly dissolved in 0.1 M HNO_3. Then 0.1 N NaOH was used to titrate this mixture to pH 10. At high pH the PVP block in PBA−$PVPH^+$ and $PVPH^+$−PEO are deprotonated but PEO is a hydrophilic polymer that stabilizes the final micelle. During the titration process of PBA−$PVPH^+$ with added PVP−PEO a three-layer "onion type" micelle is formed while for pure PVP−PEO a simple micelle is formed.[6b]

Fluorescence Measurements of the Release. The integrated steady-state fluorescence spectrum was measured on a SPEX DM3000F fluorometer as a function of time after micelle dilution to monitor the release of fluorescence probes. The chromophores used in these studies were zone-refined samples of phenanthrene and recrystallized pyrene. Each loaded micelle sample was diluted into a pair of fluorescence cells filled with aqueous solutions (water, in the case of latexes, and an appropriate buffer, in the case of micelles), one with and one without the quencher, $TlNO_3$ (0.011 M). For the PS−PMA micelles, a pH 7 phosphate buffer, composed of 0.1 M NaH_2PO_4 and Na_2HPO_4 salts, was used as the dilution medium. Studies of latex particles were carried out in pure water because buffers or significant ionic strength causes the latex particles to aggregate. For the PBA−$PVPH^+$ micelles the dilution solution was 0.1 M HNO_3 and for the PBA−PVP/PVP−PEO "onion" micelles the solution pH was 10 with 0.10 M added $NaNO_3$.

Dilution lowers the chemical potential of the probe in the solvent phase and triggers the release process, which eventually restores the equilibrium distribution of the probe. The Tl^+ quenches only that fraction of the chromophores outside the core and the "inner corona" (see later discussion). The method for relating the changes in the steady-state fluorescence intensity to the fraction of probe released with time was first used by Arca et al.,[7] and will be described below. The dilution factor chosen depended on the sample and typically ranged between 150 and 1500, to obtain an appreciable dynamic range for a given release experiment. To check for any instrumental drifts, fluorescence standards were measured at the same time as the sample although this was found not to be important for the time scales used in the data analysis. All spectra were obtained in the SPEX S/R mode to compensate for any short-term lamp fluctuations.

Experimental Results

Our results comprise three independent studies: (1) determination of the solubilization of different probe/polymer combinations; (2) determination of the fraction of probe that is accessible to the Tl^+ quencher; (3) the time-dependent release profile.

Fluorescence Measurement of Fluorophore Loading. Because the absolute concentration of the fluorescent probe is so small, it was convenient to use a fluorescence technique to determine the concentration in various solutions. The method was the following. An aliquot of the probe-saturated solution (typically 20 or 200 μL for the micelle solution or pure buffer, respectively) was added to dioxane, which dissolved the polymer latex or micelle completely. The fluorescence intensity was compared to a calibration curve for the fluorophore in dioxane (it was verified that trace amounts of water do not affect this calibration curve). The distribution coefficient for the probe was determined from

$$K_D^0 = \frac{I_{fl}^{micelle} - I_{fl}^{buffer}}{I_{fl}^{buffer}} = \frac{m_{micelle}}{m_{buffer}} \qquad (1)$$

where m_i corresponds to the number of moles of the probe in the i-th phase. It is understood that the nature of the buffer depends on the particular micelle (or latex). The superscript 0 refers to the distribution coefficient of the initial stock solution. The partition coefficient is given by

$$K_P^0 = K_D^\circ \frac{V^0_{buffer}}{V^0_{micelle}} \qquad (2)$$

where V^0_{buffer} and $V^0_{micelle}$ corresponds to the volume of the buffer solution and micelle in the solution. The volume ratio in eq 2 was taken to be equal to the mass ratio of the two phases. After dilution of the micelle solution and equilibration, the distribution coefficient may be estimated by

$$K_D^\infty = K_D^0 \frac{V^0_{buffer}}{V^\infty_{buffer}} \qquad (3)$$

where V^∞_{buffer} corresponds to the final volume in the diluted solution. This expression assumes that the probe concentration has not perturbed the micelle structure and that the partition coefficient is independent of probe concentration. We collect the values of K_D° for different probes and solutions in Table 1.[18] The mole fraction of probe in the buffer before dilution is given by $(K_D^\circ + 1)^{-1} \equiv x_{buffer}^0$, which is no larger than 0.026 (Table 1). The solubility values we obtain for the probes in pure water are in fair agreement with literature values. According to Yalkowsky and Banerjee[19] and Pearlman et al.[20] the solubility of phenanthrene in water is 6.8×10^{-6} and 7.2×10^{-6} M (both values represent an average of several reports in the literature), while we obtain 4.8×10^{-6} M. For pyrene the two literature values are 0.38×10^{-6} and 0.72×10^{-6} M, respectively. Our value agrees well with the former. We cannot account for the discrepancy between the two reference values. The main point of our solubility studies is to illustrate the relatively large amount of probe in solubilized by the micelle or latex.[21] The PVP−PEO micelle is relatively ineffective at pyrene solubilization. This is consistent with the conclusion of studies by Winnik et al. of pyrene in films composed of polystyrene-*block*-poly(vinylpyridine).[22] These workers concluded that pyrene is found almost exclusively in the polystyrene domains. In an aqueous environment, the PVP phase will be swollen, and our release studies discussed later demonstrate that pyrene diffuses out of these micelles very quickly. Because the release from PVP−PEO micelles is so fast, we did not characterize them with respect to solubilization of phenanthrene.

Determination of the Fraction of Probe Accessible to Quencher after Release. If a fluorophore is distributed in two environments, one accessible to a quencher and one inaccessible, then the fluorescence quenching should obey the following expression:[23]

$$\frac{I_0}{I_0 - I_Q} = A + \frac{A}{K_Q[Q]} \qquad (4)$$

I_0 and I_Q are the fluorescence intensities for the unquenched and quenched solution, respectively. A is given by

$$A = \frac{x_{core} + (\phi_{fl}^{buffer}/\phi_{fl}^{core})(1 - x_{core})}{(\phi_{fl}^{buffer}/\phi_{fl}^{core})(1 - x_{core})} \qquad (5)$$

Table 2. Fluorescence Quenching

sample (dilution factor)	probe	x_{core}^{∞} [a]	K_Q	b[b]	$K_D^{\infty}/(1+K_D^{\infty})$[c]
PS−PMA (300)	pyrene	0.87 (0.86)	574	1.07 ± 0.07	0.686
PS−PMA (300)	Phen	0.36 (0.44)	94.7	0.715 ± 0.105	0.525
PS latex (1500)	pyrene	0.68 (0.67)	374	1.04 ± 0.21	0.276
PS latex (300)	Phen	0.56 (0.69)	119	0.573 ± 0.125	0.421
PBA−$PVPH^+$ (1500)	pyrene	0.29 (0.44)	603[e]	0.529 ± 0.030	0.196
PBA−$PVPH^+$ (150)	Phen	0.11 (0.21)	96.1	0.483 ± 0.127	0.507
PVP−PEO (150)	pyrene	*d* (0.053)	587	*d*	0.085
PBA−PVP/PVP−PEO (1500)	pyrene	0.12 (0.17)	651	0.679 ± 0.120	0.056
PBA−PVP/PVP−PEO (150)	Phen	0.031 (0.074)	114.5	0.403 ± 0.029	0.202

[a] See eq 5 which may be inverted to yield $x_{core} = (A-1)/(A+(1-b)/b)$. Value in (parentheses) computed for $b = 1$, where $b = \phi_{fl}^{buffer}/\phi_{fl}^{core}$. [b] See eq 13. Average value from three release experiments and the independent values of the slope and intercept. [c] This value should agree with x_{core}^{∞} if K_D obeys a simple dilution relation (eq 3) and if all solubilized probe is protected from the Tl^+ quencher (see the discussion following eq 8). [d] Since release experiments could not be carried out with this system, no *b* value was obtained. [e] The fit to eq 4 was not as good as the other cases, perhaps because of probe quenching by $PVPH^+$ groups.

and later we denote the ratio of quantum yields $\phi_{fl}^{buffer}/\phi_{fl}^{core}$ as *b*. In this expression x_{core} is the mole fraction of the probe that resides in the micelle "core", which *by definition* is inaccessible to the ionic quencher Tl^+. The inner portion of the corona may contain probe which may not be accessible to Tl^+ because of chain crowding and repressed ionization.[24] The ratio of the fluorescence quantum yields of the probe in the "core" and in the buffer is a weighted average for the probe inside the core and inner corona (ϕ_{fl}^{core}) and in the bulk solution and the accessible outer corona (ϕ_{fl}^{buffer}). If this ratio is unity one recovers the normally quoted result

$$A = \frac{1}{1 - x_{core}} \tag{6}$$

where *A* is the inverse of the mole fraction of accessible fluorophores. K_Q is the Stern−Volmer quenching constant for the accessible fluorophores. By fitting fluorescence quenching data to eq 4 and independently determining $\phi_{fl}^{buffer}/\phi_{fl}^{core}$ ($\equiv b$; see next section), we can obtain x_{core}. These values are presented in Table 2.

If the distribution coefficient is independently known and does not depend on the probe concentration, then one can estimate the fraction of the probe that resides "within the micelle corona", which *by definition* is accessible to the quencher. Using the expression for the distribution coefficient

$$K_D = \frac{x_{core} + x_{corona}}{x_{buffer}} = \frac{1 - x_{buffer}}{x_{buffer}} \tag{7}$$

one may derive

$$x_{corona} = \frac{K_D}{1 + K_D} - x_{core} \tag{8}$$

x_{core} is obtained from the quantity *A* obtained from the quenching experiment and knowledge of *b* (eq 5). The following experiment was carried out: The stock solution of micelles was diluted and allowed to equilibrate. Equation 3 was used to compute K_D^{∞} and x_{core}^{∞} is obtained from eq 5, with and without the correction for *b*. These data are presented in Table 2. A larger fraction of the probes remain in the core after equilibration for the polystyrene cores than for poly(*tert*-butyl acrylate), but this is also dependent on the dilution factor. The smallest value of x_{core}^{∞} is obtained for pyrene in PVP−PEO, which also has the smallest value of $K_D°$.

Scheme 1

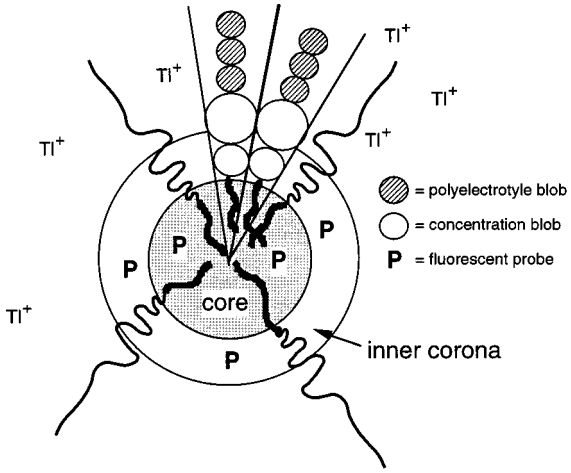

While there is significant experimental error in x_{core}^{∞}, the computed values of x_{corona}^{∞} computed from eq 8 are negative for pyrene (e.g., compare columns 3 and 6 of Table 2), which has no physical meaning. This suggests that there is either (1) a concentration effect on $K_D°$, or (2) most of the probe that is solubilized by the micelle is also protected from the Tl^+ ion, or both. For phenanthrene in PBA−$PVPH^+$ or PBA−PVP/PVP−PEO a positive x_{corona}^{∞} value is obtained from eq 8. This would suggest that a significant fraction of the phenanthrene probes are located in a relatively swollen part of the PVP corona that can be reached by the Tl^+ ion. These differences illustrate the degree of chemical specificity that might be present in solubilization by polymer micelles.

As we will see later, there is a significant fraction of solubilized probe that is released rapidly upon dilution. We assign this fraction to the "inner corona" of the micelle (or in the case of the latex particle, preferential surface adsorption) and we propose that diffusion of the probe from this region is rapid. Our physical model is illustrated in Scheme 1. As noted earlier, this is similar to the conclusion of Winnik et al. for a similar polymer system but a very different probe.[14]

Release Profiles Generated from Fluorescence Data

General Method. The dilution of the loaded micelle or latex sample initiates the release process which can be monitored by changes in the fluorescence intensity with time. Figure 1 illustrates an example of the fluorescence as a function of time for pyrene released from PS−PMA in the absence ($I_U(t)$) and presence ($I_Q(t)$) of the quencher, Tl^+. A simple two state model approach to the fluorescence data is used,[7] whereby the total fluorescence is assumed to be the sum of the contributions in the "core" and buffer phases: $I(t) =$

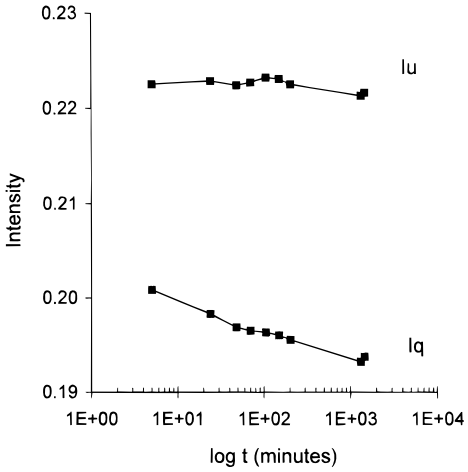

Figure 1. Quenched ($I_Q(t)$) and unquenched ($I_U(t)$) fluorescence intensities after the initial injection of a pyrene-loaded PS−PMA micelle solution into buffer, in the presence of 0.011 M $TlNO_3$.

$I_{core}(t) + I_{buffer}(t)$. $I_{core}(t)$ represents the unquenchable fraction of the probes, which may include the inner corona, and $I_{buffer}(t)$ may include some probe in the outer corona, which can be quenched. The fluorescence contribution from the i-th phase is given by

$$I_i = kCx_i\phi_{fl}^{\ i} \tag{9}$$

where k is an instrumental constant, C is the total chromophore concentration, and ϕ_{fl}^{i} is the quantum yield of the chromophore in the i-th phase. x_i is the mole fraction of the total chromophore population in the i-th phase. The total fluorescence intensity in the unquenched sample can then be expressed in terms of the fractions of the chromophore population in the core and solvent phases:

$$I_U(t) = I_{core}(t) + I_{buffer}(t) \tag{10a}$$

$$= kC\{x_{core}(t)\phi_{fl}^{\ core} + x_{buffer}(t)\phi_{fl}^{\ buffer}\} \tag{10b}$$

$$= kC\phi_{fl}^{\ core}\{x_{core}(t) + (1 - x_{core}(t))b\} \tag{10c}$$

$x_{core}(t) + x_{buffer}(t) = 1$ and $b = \phi_{fl}^{buffer}/\phi_{fl}^{core}$ is the ratio of the chromophore quantum yields. In the presence of an aqueous quencher which is completely inaccessible to the core phase, the analogous expression for the quenched solution is given by

$$I_Q(t) = kC\phi_{fl}^{\ core}\{x_{core}(t) + (1 - x_{core}(t))bq\} \tag{11}$$

where $q = I_Q/I_0$ is the independently measured ratio of the quenched to unquenched fluorescence intensity in the buffer phase alone. Alternatively, according to the derivation that leads to eq 4, q is given by

$$q = \frac{1}{1 + K_Q[Q]_R} \tag{12}$$

where $[Q]_R$ is the quencher concentration used in the release experiment. These equations assume that the fluorescence intensities of the quenched and unquenched samples differ only in the contribution from the bulk solvent phase (the solvent phase fluorescence intensity for the quenched sample has been lowered by a factor q).

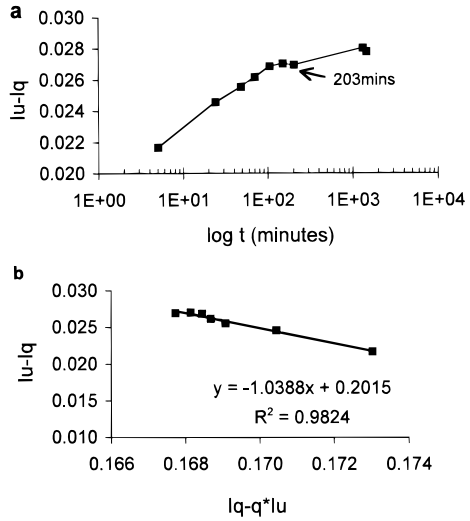

Figure 2. (a) Plot of $I_U(t) - I_Q(t)$ vs time (see eq 15 of text) or (b) $[I_Q(t) - qI_U(t)]$ (see eq 13 of text) for the release of pyrene from PS−PMA micelles into buffer. The former plot illustrates the loss of pyrene to the cell walls at longer times. The latter plot illustrates the method for determination of b and $kC\phi_{fl}^{core}$.

The elimination of $x_{core}(t)$ from eqs 10 and 11 yields

$$I_U(t) - I_Q(t) = kC\phi_{fl}^{\ core}b(1 - q) - b[I_Q(t) - qI_U(t)] \tag{13}$$

The quantum yield ratio, b and the constant $kC\phi_{fl}^{core}$ can be obtained from the slope and intercept, respectively, of a plot of $I_U(t) - I_Q(t)$ vs $I_Q(t) - qI_U(t)$. Figure 2 illustrates an example of this plot for the case of pyrene released from PS−PMA.

The fraction of chromophores remaining in the core as a function of elapsed time is then given by eliminating I_U:

$$x_{core}(t) = \frac{I_Q(t) - bqkC\phi_{fl}^{\ core}}{kC\phi_{fl}^{\ core}(1 - bq)} \tag{14}$$

A release profile can then be generated by plotting the fraction in the buffer phase, $x_{buffer}(t) = 1 - x_{core}(t)$ vs time as illustrated in Figure 3 for the case of pyrene released from a PS−PMA micelle. As will be discussed in more detail later, essentially all the probe is confined to the micelle in the injected solution (see $x_{buffer}^{\ 0}$ values in Table 1). The initial difference in $I_Q(t)$ and $I_U(t)$ is complete in tens of seconds so there is a very rapid release of the probes from the micelle followed by the much slower release which is followed and analyzed by our experiments.

According to eqs 10c and 11

$$I_U(t) - I_Q(t) = kC\phi_{fl}^{\ core}b(1 - q)(1 - x_{core}(t)) \tag{15}$$

Therefore $I_U(t) - I_Q(t)$ must increase toward a final limiting value unless the total concentration of probe (C) decreases. In fact in some cases we find $I_U(t) - I_Q(t)$ decreases at longer times (ca. 3−5 h), which must be the result of adsorption of the probe onto the walls of the fluorescence cells. Independent measurements have demonstrated that the loss of probe is not a photochemical process, and in any case the exposure of the solution to light is minimized. In the analysis

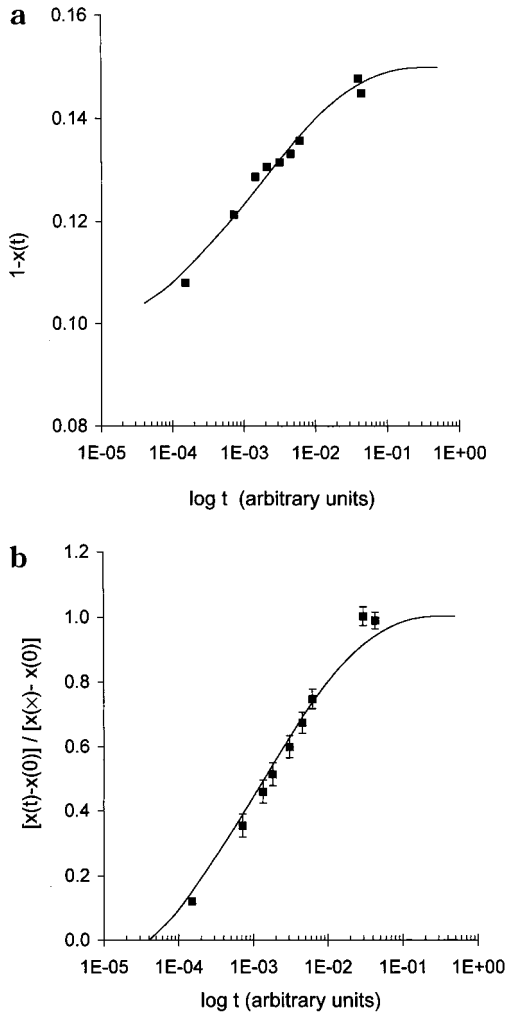

Figure 3. (a) Released fraction, $x_{buffer}(t)$, of pyrene from PS−PMA plotted as function of log time (in arbitrary units). The fit to the model is also given. (b) Release normalized according to eq 17, averaged for three independent experiments, with the same fit to the model.

described next we consider only the time range for which $I_U(t) - I_Q(t)$ is increasing.

Diffusion-Controlled Release from a Sphere. In this model it is assumed that the diffusion in the sphere is purely radial and that the diffusion coefficient is constant. The diffusion can then be described by Fick's second law

$$\frac{\partial C}{\partial t} = D\left\{\frac{\partial^2 C}{\partial^2 r} + \frac{2\partial C}{r\partial r}\right\} \tag{16}$$

A solution is presented by Crank for diffusion out of a simple sphere of radius R_s into a finite volume for the case that the initial concentration inside the sphere is uniform and the concentration in the outer phase is maintained uniform at all times (a stirred solution)[25]

$$\frac{x(t) - x_0}{x_\infty - x_0} = 1 - \sum_{n=1}^{\infty}\left[\frac{6\alpha(\alpha+1)}{9 + 9\alpha + q_n{}^2\alpha^2}\right]\exp(-q_n{}^2 Dt/R_s{}^2) \tag{17}$$

where $x(t)$ is the mole fraction in either phase and α corresponds to $(K_D^\infty)^{-1}$, the distribution coefficient at equilibrium of the diluted solution. The quantities q_n are the nonzero solutions to the equation

$$\tan(q_n) = \frac{3q_n}{3 + \alpha q_n{}^2} \tag{18}$$

The values of q_n depend on α. The first few values are in the ranges 3.14−4.19, 6.28−7.73, and 9.42−10.9 for K_D^∞ from zero to infinity,[26] so the dependence of eq 17 on K_D^∞ is weak. We choose to present our data as $x_{buffer}(t) = 1 - x_{core}(t)$. According to Crank the fraction remaining in the sphere at infinite time is given by

$$\frac{x_\infty}{x_0} = \frac{K_D{}^\infty}{1 + K_D{}^\infty} \tag{19}$$

where x_0 is essentially unity because the fraction of probe in the bulk solution in the initially injected samples represents no more than a few percent of the total (see next paragraph). In our analysis of the time dependent release using eq 17, x_0 is taken to be the fraction of probe that remains in the core after the initial burst release, $1 - x_{buffer}(0)$ (see later). For the purpose of comparing the results of Fick's law with the experimental release data, it was found to be more convenient to solve the diffusion equation numerically using a finite difference method. The description of the method is given elsewhere and is found to be in excellent agreement with the analytical solution.[7,27]

From the experimental release profile we obtain a value of $x_{buffer}(0)$ at the earliest time possible with our technique (ca. 60 s mixing, followed by a 1−2 min fluorescence scan, depending on the sample). To monitor the fluorescence on shorter time scales the intensity at a single wavelength can be followed as a function of time after injection. As stated earlier, the initial fast release is complete in less than 30 s.[28] $x_{buffer}(0)$ is much larger than expected from the fraction of probe in the buffer phase ($x_{buffer}{}^0$ in Table 1). This is consistent with our model for the micelle in which a significant fraction of the probe is contained within the inner part of the micelle corona, where it is protected from Tl^+ quenching but where the diffusion constant is much larger than for the glassy core. After this initial "burst release" the diffusion is much slower and is fit satisfactorily to diffusion from a sphere (see later). As can be seen from eq 17, the time dependence of release depends on $D/r_{core}{}^2$ (r_{core} replaces R_s) and K_D^∞. In our previous work we obtained K_D^∞ from the best fit of the data to the kinetic model. However the shape of the computed release curve in the form presented in eq 17 is not very sensitive to K_D^∞. Therefore our analysis of the data is as follows.

(1) From the fluorescence intensity measured at the earliest time, we estimate $x_{buffer}(0)$ as an independent parameter that cannot be computed from $K_D°$ (eq 3) or the fluorescence quenching (eq 5). $x_{buffer}(0)$ is determined primarily by the fraction of the probe that resides in the "inner corona" according to our model.

(2) The normalized release curve (eq 17) is computed using the K_D^∞ value calculated from eq 3 or estimated from the best fit. The shape of this curve is not very sensitive to K_D^∞, which is fortunate because it is the time shift parameter (see below) that yields $D/r_{core}{}^2$.

(3) The $x_{buffer}(t)$ data from eq 14 are used only over the time scale for which $I_U(t) - I_Q(t)$ is increasing (see eq 15). After this time the probe is being lost to the cell walls and the assumptions of the model are no

Table 3. Release Kinetics Results

sample[c]	probe	$x_{buffer}(0)$	$\Delta\tau_{expt} = r_{core}^2/D$ (s)[b]	r_{core} (nm)	D (cm^2/s)[b]
PS−PMA	pyrene	0.064 (±0.04)	2.2 (±0.8) × 10^6	14.4[a]	9.4 (±3.5) × 10^{-19}
	Phen	0.37 (±0.05)	2.0 (±0.5) × 10^5		1.0 (±0.3) × 10^{-17}
PS latex	pyrene	0.18 (±0.05)	7.8 (±2.6) × 10^6	32	1.3 (±0.5) × 10^{-18}
	Phen	0.37 (±0.05)	8.6 (±3.0) × 10^5		1.2 (±0.5) × 10^{-17}
PBA−PVPH$^+$	pyrene	0.59 (±0.07)	2.9 (±0.5) × 10^4	14.3[a]	7.0 (±1.3) × 10^{-17}
	Phen	0.64 (±0.03)	6.8 (±0.9) × 10^3		3.0 (±0.4) × 10^{-16}
PBA−PVP/PVP−PEO	pyrene	0.62 (±0.03)	3.2 (±1.1) × 10^4	14.3[d]	6.4 (±2.5) × 10^{-17}
	Phen	0.78 (±0.05)	9.3 (±1.8) × 10^3		2.2 (±0.4) × 10^{-16}

[a] Estimate of the micelle core radius, r_{core}, based on eq 21. [b] See text, eq 20. [c] Dilution factor same as Table 2. [d] See text; this assumes the core of the onion micelle to be the same as the PBA−PVPH$^+$ micelle.

longer valid. Of course some loss to the cell walls occurs over all time scales, but this is a minor contribution to the loss of fluorescence signal at the earlier times of the experiment. It was verified that this effect is minor by a separate "takeup" experiment described later.

(4) The plot of $x_{buffer}(t)$ or $(x_{buffer}(t) - x_{buffer}(0))/(x_{buffer}^{\infty} - x_{buffer}(0))$ as a function of log t is compared to the computed release curve which is a function of the dimensionless parameter Dt/r_{core}^2. The time shift required to achieve the best fit between the data ($\Delta\tau_{expt}$) and the model calculation yields the relationship

$$\Delta\tau_{expt} = r_{core}^2/D \tag{20}$$

If we have knowledge of r_{core}, D can be evaluated. The radius of the micelle core, r_{core}, is estimated assuming an impenetrable sphere:

$$r_{core} = \left[\frac{3M_{micelle}W_{core}\nu_{core}}{4\pi N_A \Phi_{core}}\right]^{1/3} \tag{21}$$

In eq 21 $M_{micelle}$ is the micelle molecular weight, W_{core} is the weight fraction of the core copolymer, ν_{core} is the specific volume of the core polymer, and Φ_{core} (assumed to be unity) is the polymer volume fraction in the micelle core (i.e., penetration of the core by water is ignored). These values are collected in Table 3. As stated above, the time shift is not very sensitive to K_D^{∞}. The combined uncertainty in $\Delta\tau_{expt}$ is of the order of ±20% based on multiple release experiments with independent fits of the data. We emphasize that the D values we obtain apply only to the slow portion of the release. While a satisfactory fit to a homogeneous sphere model is obtained, these release curves are not sufficiently sensitive to test modifications of the model, such as the effect of small inhomogeneities in loading (if any), concentration dependent diffusion constants, finite size effects, etc. We did verify that we can easily distinguish a zeroth order release profile from diffusive release from a sphere.[29] Also the reasonable agreement between the PS−PMA micelle and the PS latex diffusion constants (Table 3) despite the significant different in r_{core} values implies that the process we are characterizing is a diffusive process.

The PS−PVP/PVP−PEO micelle is believed to have a concentric sphere ("onion skin") morphology, and hence one might expect different diffusion constants for the two layers. It is easy to solve the diffusion equation for concentric spheres numerically. We find that the diffusion constants for the two layers must be quite different before the release curve is distinct from the simple sphere model and then only if the outer sphere has a much lower diffusion constant than the inner sphere (which corresponds to a zeroth order release[29]). Within the accuracy of our fitting procedure, we cannot distinguish the simple sphere from the concentric sphere model, so we use the former to fit data for the "onion skin" micelles as well. We will argue later that the diffusion constant for the outer sphere is larger than that of the inner sphere.

Effect of Added Ionic Strength. The distribution of quencher is an important consideration when analyzing the release from micelle data. Although the polyelectrolyte corona is quite different from solutions of linear polyelectrolytes, the influence of ionic strength on the counterion distribution cannot be neglected. The Tl^+ ions can preferentially associate with the micelle's polyelectrolyte-type corona in solutions of the PS−PMA micelle in pure water. When the release from PS−PMA was measured using pure water as the dilution medium, the quenched sample exhibited an initial decrease in the fluorescence intensity followed by a gradual increase (data not shown). This behavior is attributed to the transport of chromophores from the micelle core to the corona, which has a high local Tl^+ concentration. As the chromophore leaves the corona to a higher quantum yield environment of the solvent, where the Tl^+ quencher is relatively depleted, the fluorescence increases. If a pH 7, 0.1 M phosphate buffer is used as the dilution medium, this effect is eliminated. For the PBA−PVPH$^+$ micelles the cationic corona repels the Tl^+ but from independent experiments we know that protonated linear PVPH$^+$ quenches the fluorescence of covalently bound chromophores.[30] We do not observe any obvious effect of quenching by the corona for PBA−PVPH$^+$.

Takeup Experiments

To verify that our method of loading the micelles and/or the assumption that we could ignore long time data which is distorted by loss of probe to the cell walls, the following experiment was carried out: an aqueous solution (with or without Tl^+ quencher) was saturated with pyrene. The fluorescence cell cap was modified to permit a roughened glass rod to extend into the solution without interfering with the excitation beam. This glass rod was coated with pyrene by being dipped into an organic solution of pyrene and air-dried. Thus this rod is a reservoir of pyrene that will maintain a constant pyrene concentration in the aqueous phase. While observing the fluorescence of the stirred solution 20 μL of a 2 mg/mL of pyrene-free PS-*b*-PMA micelle was injected. The fluorescence immediately increased, followed by a much slower increase that was monitored for approximately 24 h. This increased fluorescence can be ascribed to additional pyrene that is solubilized by the micelle. If Tl^+ is present, the increase is more dramatic because the pyrene in the bulk phase is significantly quenched (we use the same Tl^+ concentration as in the release experiments). The spectrum itself also changes dramatically in the presence of Tl^+ because

of the well-known sensitivity of pyrene fluorescence to polarity.[4h,31,32] The increase in fluorescence can be treated by an equation that is equivalent to eq 17.[33] The time-shift parameter agrees with that obtained from the release experiments within experimental error. Therefore we conclude that, within the experimental precision of this experimental method, the diffusion constant we obtain is not influenced by our loading method and that the loading is not plasticizing the micelle core.[34] We emphasize that the accuracy of our method is not so high (sometimes there is 50% uncertainty in the estimated diffusion constants in Table 3), and it is the large differences between the various core−probe combinations we wish to emphasize, as well as the very small values of D we are able to measure. The general agreement between release and takeup experiments is consistent with the results from pyrene−perylene exchange between micelles.[8]

Analysis of the Experimental Release Data

An example of the time dependent fluorescence signals ($I_U(t)$ and $I_Q(t)$, see eqs 10 and 11) is presented in Figure 1 for PS−PMA micelle with pyrene as the probe. As can be seen from Figure 2, after 203 min the slope of $I_U(t) - I_Q(t)$ changes sign, implying that loss of the probe to the cuvette walls plays a significant role in the fluorescence intensity.[35] The plot of the data according to eq 13 is presented in Figure 2, from which b is extracted. This plot only includes the data to 203 min. In general, the time points for which $I_U(t) - I_Q(t)$ decreases are excluded from the analysis but this does not occur for this particular data set out to 10^3 minutes (16.7 h). The release profile $x_{buffer}(t)$ ($=1 - x_{core}(t)$) is plotted as a function of log time in Figure 3, along with the best fit to the model of diffusion from a sphere. For comparison the release plotted according to eq 17 is also given. As discussed in an earlier section, we prefer this form of a plot because it minimizes the sensitivity of the fit to the choice of K_D^∞ and $x_{buffer}(0)$. However, the values of the time shift ($\Delta\tau_{expt} = r_{core}^2/D$, eq 20) obtained from either type of plot are always in reasonable agreement. Similarly, if we analyze the averaged release curves, we obtain essentially the same values of $\Delta\tau_{expt}$. We find that $\Delta\tau_{expt}$ is not particularly sensitive to the values of q, b, $x_{buffer}(0)$, and K_D^∞ because the primary feature of the release curve that determines $\Delta\tau_{expt}$ is the time at which there is maximum curvature.

The data analysis for all systems is carried out in a similar fashion and the values of $x_{buffer}(0)$ and $\Delta\tau_{expt}$ are collected in Table 3. One exceptional case was the PVP−PEO micelles. In this case the release was so fast that no change in $I_U(t) - I_Q(t)$ could be detected after mixing and placing the solution in the fluorometer. We ascribe this observation to the fact that water swells poly(2-vinylpyridine), which diminishes its solubilization capacity and will increase the diffusion constant of a small molecule probe. For this reason we use the same r_{core} value for the PBA−PVP/PVP−PEO "onion" micelle as for PBA−PVPH$^+$ in the calculations of D, and with this assumption, the diffusion constants for these two systems agree within their standard deviations. If we chose to use a larger r_{core} value for the onion micelle, then the calculated diffusion constant, which represents a weighted average of the two phases, will be larger. As discussed earlier, if one models diffusion from concentric spheres, there is essentially no difference in the release profile compared to the single sphere model unless the outer sphere has a substantially lower diffusion constant than the inner sphere, which is the opposite of the present situation.

Qualitatively the diffusion constants behave as expected.

(1) The diffusion constant for pyrene is substantially smaller than that of phenanthrene (a factor of ca. 10 in polystyrene, a factor of ca. 4 for poly(*tert*-butyl acrylate)). This is expected given the exponential dependence of the diffusion constant on molecular size[36] (the molecular volumes are 186 and 169.5 Å^3 for pyrene and phenanthrene, respectively[20]).

(2) The diffusion constant of a given probe is smaller in polystyrene than in PBA by a factor of ca. 60 for pyrene and 24 for phenanthrene. This correlates qualitatively with the T_g values (cf. 373 and 313−316 K for PS and PBA, respectively[37]).

The absolute values of the diffusion constants we obtain with our methods are exceptionally low. While it is plausible that these values would be appropriate for the same probes in bulk polymers at room temperature, the fact that we are studying micelle cores that are not so much larger than the polymer chain dimension could modify the transport properties. Most studies we are aware of are for smaller probes[36] or at temperatures much closer to T_g.[38]

The values of $x_{buffer}(0)$ in Table 3 should be noted. They are all much larger than the value of x_{buffer}^0 computed from the independently measured distribution coefficient, $K_D°$ (Table 1, column 4). From the quenching experiments the comparison of x_{core}^∞ and $K_D^\infty(1 + K_D^\infty)^{-1}$ (Table 2) suggests that most if not all of the solubilized probe is protected from the Tl^+ quencher. Hence we ascribe the "burst release" represented by $x_{buffer}(0) - x_{buffer}^0$ to the "inner corona" of the micelle or the outer portion of the latex particle. The values of $x_{buffer}(0)$ are particularly large for the PBA−PVPH$^+$ or PBA−PVP/PVP−PEO micelles. We postulate that a significant fraction of the probe molecules are solubilized by the PVP inner corona and are rapidly released because of the rubbery nature of the swollen PVP.

The values of $x_{buffer}(0)$ is much larger for phenanthrene solubilized by PS−PMA than pyrene. We presume this reflects the enhanced solubilization of phenanthrene by protonated methacrylic acid groups of the inner corona compared to the more hydrophobic pyrene. We are not aware of any study of the relative solubilization of phenanthrene and pyrene by linear PMA at low pH, which we regard as an approximate model for the inner corona.

The interpretation of $x_{buffer}(0)$ for the PS latex is necessarily different than for the micelle, and would have to be ascribed to "surface absorption". We miss the earliest part of the release with our experimental technique (e.g., a dead time of ca. 200 s before the first data point is collected). This would correspond to a movement of ca. 1.6 and 4.9 Å for pyrene and phenanthrene, respectively (estimated by $\sqrt{200D}$). Thus the $x_{buffer}(0)$ for PS latexes must represent probes that reside in a polymer−water interface that protects the probe from the Tl^+ ions but has a much larger probe diffusion constant than the interior of the latex particle. This implies a less dense polystyrene structure near the interface, analogous to the "inner corona" model. We are not aware of any other experiments that support or refute this picture of a "fuzzy" PS−water interface. However, Bergbreiter et al. have proposed a similar

picture for the interface between high-density polyethylene and organic solvents based on the fluorescence quenching of surface pyrene groups.[39]

We should point out that our measurement of a finite rate of pyrene migration out of our polymer micelles stands in contrast to the report of Creutz et al.[12] In these papers the objective was to measure the rate of polymer chain exchange between micelles using naphthalene-tagged poly((dimethylamino)ethyl methacrylate)-*b*-poly(sodium methacrylate) mixed with untagged polymer micelles but containing dissolved pyrene. As part of their analysis they conclude that no pyrene diffuses out of their micelles over a 2 h period. For all of our polymer micelles a substantial fractional release occurs over this time period, so we conclude that there must be specific attractive interactions between the poly((dimethylamino)ethyl methacrylate) core and pyrene.

Summary

The primary objective of this paper is the characterization of the release kinetics of two hydrophobic probes (pyrene and phenanthrene) loaded into various polymer micelles. Polystyrene latex particles were also characterized for comparison. The polymer micelle cores were composed of polystyrene, poly(*tert*-butyl acrylate), and poly(2-vinylpyridine). The last polymer is swollen by water, and the release rate was too fast to be observed by our techniques. The diffusion constants for the first two cases were very small (10^{-18}−10^{-16} cm^2/s), depending on the core and probe (Table 3).

Independent measurements of the partition coefficient of the probes between the micelle and water demonstrated that in general the micelles are very effective at solubilization (partition coefficients from 4×10^4 to 3×10^5 were obtained, depending on the micelle−probe combination; see Table 1 for K_P^0 values). This permits a comparison of the fraction of probe released at the earliest time, $x_{buffer}(0)$, and the amount of probe present in the bulk solution of the stock solutions before dilution, x_{buffer}^0. $x_{buffer}(0)$ is much larger than x_{buffer}^0, so we conclude that a significant fraction of the probe is solubilized in the corona, which because of its swollen state permits the rapid diffusion of the probe into the bulk solution. By examining the fluorescence quenching of the solubilized probe, we conclude that essentially all solubilized probe is protected from the Tl^+ quenching ion. On the basis of these observations, we propose that the micelle can be thought of as having three regions: (1) the core, which for our systems is glassy (except for the PVP−PEO micelle); (2) an "inner corona", composed of the hydrophilic block polymer, which may be swollen by water but where the ionization by gain or loss of protons is suppressed (the polymer density is sufficiently high in this region that simple ions such as Tl^+ do not penetrate[40] and where, for a cation micelle like PBA−$PVPH^+$ we do not expect Tl^+ to penetrate the corona in any case); (3) an "outer corona" for which the chains are not crowded and which may sustain a significant charge density. This model is consistent with some theoretical predictions[24,41] and is illustrated in Scheme 1. Scheme 1 is also a good representation of the situation for the "onion micelles", except the role of the "inner corona" is played by the swollen PVP chains and the "outer corona" is composed of the PEO chains. The important role of the corona in solubilization was not appreciated by us in our earlier study of phenanthrene released from two different PS−PMA micelles.[42]

We have not explored the effect of the probe loading, because we have endeavored to saturate our particles. The weight percent of the probes in the micelles is not particularly high (e.g., 3 and 9 wt % for pyrene and phenanthrene in PS−PMA). For solubilization in the corona, one might expect the probe to affect the local structure because of its strongly hydrophobic nature. Smaller probe molecules would be expected to plasticize the micelle core, such that the effective diffusion constant would change as the release proceeded. We would not expect to observe this effect with our technique because the precision of the fit to the theoretical model is not adequate to detect such subtle effects.

Acknowledgment. This work has been supported by the U.S. Army Office of Research (Grant DAAH04-95-1-0127) and the Robert A. Welch Foundation (F-356).

Supporting Information Available: The following data are given for each micelle/latex sample with pyrene and phenanthrene probes: (1) the averaged, normalized release plotted like eq 17 vs log time including the best fit to the diffusion from a sphere; (2) a plot of $1 - x(t)_{micelle}$ vs t; (3) typical plots of the quenched ($I_Q(t)$) or unquenched ($I_U(t)$) fluorescence intensity vs time (15 pages). Ordering and accessing information is given on any current masthead page.

References and Notes

(1) (a) Tuzar, Z.; Kratochvil, P. In *Surface and Colloid Science*; Matijevic, E. Ed.; Plenum Press: New York, 1993: Vol. 15, p 1. (b) Riess, G.; Hurtrez, G.; Bahadur, P. In *Encyclopedia of Polymer Science and Engineering*, 2nd ed.; Mark, H. F., Bikales, N. M., Overberger, C. G., Menges, G., Eds.; Wiley: New York, 1985; Vol. 2, pp 324−436. (c) *Solvents and Self-Organization of Polymers*; Webber, S. E., Munk, P., Tuzar, Z., Eds.; NATO ASI Series E 327, Kluwer Academic Publishers: Dordrecht, The Netherlands, 1996.

(2) (a) Nagarajan, R. *Curr. Opin. Colloid Interface Sci.* **1996**, *1*, 391. (b) Tian, M.; Arca, C.; Tuzar, Z.; Webber, S. E.; Munk, P. *J. Polym. Sci., B: Polym. Phys.* **1995**, *33*, 1713. Hurter, P. N.; Alexandridis, P.; Hatton, T. A. In *Solubilization in Surfactant Aggregates*; Christian, S. D., Scamehorn, J. F., Eds.; Marcel Dekker: New York, 1995; pp 191−235. (c) Gadell, F.; Koros, W. J.; Schechter, R. S. *Macromolecules*, **1995**, *28*, 4883. (d) Kabanov, A. V.; Nazarova, I. R., Astafieva, I. V.; Batrakova, E. V.; Alakhov, V. A. *Macromolecules*, **1995**, *28*, 2303. (e) Haulbrook, W. R.; Feerer, J. L.; Hatton, T. A.; Tester, J. W. *Environ. Sci. Technol.* **1993**, *27*, 2783.

(3) (a) Harada, A.; Kataoka, K. *Adv. Drug Delivery Rev.* **1995**, *16*, 295. (b) Harada, A.; Kataoka, K. *Macromolecules* **1995**, *28*, 5294. (c) Scholz, C.; Iijima, M.; Nagasaki, Y.; Kataoka, K. *Macromolecules* **1995**, *28*, 7295. (d) Bader, J. H.; Rin, H.; Schmidt, B. *Angew. Makromol. Chem.* **1984**, *123*, 457.

(4) (a) Karymov, M. A.; Procházka, K.; Mendenhall, J. M.; Martin, T. J.; Munk, P.; Webber, S. E. *Langmuir* **1996**, *12*, 4748. (b) Martin, T. J.; Webber, S. E. *Macromolecules* **1995**, *28*, 8845. (c) Qin, A.; Tian, M.; Ramireddy, C.; Webber, S. E.; Munk, P.; Tuzar, Z. *Macromolecules* **1994**, *27*, 120. (d) Chan, J.; Fox, S.; Kiserow, D. J.; Ramireddy, C.; Munk, P.; Webber, S. E. *Macromolecules* **1993**, *26*, 7016. (e) Tian, M.; Qin, A.; Ramireddy, C.; Webber, W. E.; Munk, P.; Tuzar, Z.; Procházka, K. *Langmuir* **1993**, *9*, 1741. (f) Procházka, K.; Kiserow, D.; Ramireddy, C.; Tuzar, Z.; Munk, P., Webber, S. E. *Macromolecules* **1992**, *25*, 454. (g) Kiserow, D.: Procházka, K.; Ramireddy, C.; Tuzar, Z.; Munk, P., Webber, S. E. *Macromolecules* **1992**, *25*, 461. (h) Cao. T.; Munk, P.; Ramireddy, C.; Tuzar, Z.; Webber, S. E. *Macromolecules* **1991**, *24*, 6300.

(5) Martin, T. J.; Procházka, K.; Munk, P.; Webber, S. E. *Macromolecules* **1996,** *29*, 6071.

(6) Procházka, K.; Martin, T. J.; Munk, P.; Webber, S. E. *Macromolecules* **1996**, *29*: (a) 6526; (b) 6518.

(7) Arca, E.; Tian, M.; Webber, S. E.; Munk, P. *Int. J. Polym. Anal. Charact.* **1995**, *2*, 31.

(8) (a) Stepánek, M.; Krijtová, K.; Procházka, K.; Teng, Y.; Webber, S. E.; Munk, P. *Acta Polym.* **1998**, *49*, 96. (b) Stepánek, M.; Krijtová, K.; Limpouchová, Z.; Procházka, K.; Teng, Y.; Webber, S. E.; Munk, P. *Acta Polym.* **1998**, *49*, 103.
(9) Wang, Y.; Kausch, C. M.; Chun, M. Quirk, R. P.; Mattice, W. L. *Macromolecules* **1995**, *28*, 904.
(10) Smith, C. K.; Liu, G. *Macromolecules* **1996**, *29*, 2060.
(11) Rager, T.; Meyer, W. H.; Wegner, G.; Winnik, M. A. *Macromolecules* **1997**, *30*, 4911.
(12) (a) Creutz, S.; van Stam, J.; De Schryver, F. C.; Jérôme, R. *Macromolecules* **1998**, *31*, 681. (b) Creutz, S.; van Stam, J.; Antoun, S.; De Schryver, F. C.; Jérôme, R. *Macromolecules* **1997**, *30*, 4078.
(13) Reviews include (a) Kalyanasundaram, K. *Photochemistry in Microheterogeneous Systems*; Academic Press: Orlando, FL 1987. (b) Zana, R. Ed. *Surfactant Solutions*; Marcel Dekker: New York, 1987.
(14) Hruska, Z.; Piton, M.; Yekta, A.; Duhamel, J.; Winnik, M. A. *Macromolecules* **1993**, *26*, 1825.
(15) Martin, T. J. Ph.D. Dissertation, The University of Texas at Austin, May, 1996. These micelles are similar to those studied in ref 8.
(16) Private communication.
(17) TlCl has limited solubility ($K_{sp} = 1.86 \times 10^{-4}$: *CRC Handbook of Chemistry and Physics*, 77th ed.; Lide, D. R., Ed., 1996; p 8-92), but for our HCl and Tl^+ quencher concentrations (1.0×10^{-2} and 1.1×10^{-2} M, respectively), no precipitation was observed.
(18) In ref 8 an alternative fluorescence method obtained a partition coefficient of pyrene in similar PS−PMA micelles approximately twice that obtained in this study.
(19) Yalkowsky, S. H.; Banerjee, S. *Aqueous Solubility*; Marcel Dekker: New York, 1992. See Table 4.2.
(20) Pearlman, R. S.; Yalkowsky, S. H.; Banerjee, S. *J. Phys. Chem. Ref. Data* **1984**, *13*, 555.
(21) From the relation $m_{total} = m_{micelle} + m_{buffer} = m_{buffer}(K_D^0 + 1)$, the total concentration of probe divided by $K_D^0 + 1$ should yield the aqueous solubility of the probe. We obtain $[Py]_{buffer} = 0.58 \pm 0.06$ mM and $[Phen]_{buffer} = 3.7 \pm 0.4$ mM, both of which are slightly different than the values in Table 1. These differences illustrate the accuracy of our method when applied to very dilute solutions.
(22) Nakashima, K.; Winnik, M. A.; Dai, K. H.; Kramer, E. J.; Washiyama, J. *Macromolecules* **1992**, *25*, 6866.
(23) Lakowicz, J. R. *Principles of Fluorescence Spectroscopy*; Plenum Press: New York, 1983.
(24) Lyatskaya et al. have argued that the deprotonation in micelles of this class will be a strong function of distance from the core/corona interface at low ionic strength (Lyatskaya, Y. V.; Leermakers, F. A. M.; Fleer, G. J.; Zhulina, E. B.; Birshtein, T. M. *Macromolecules* **1995**, *28*, 3562).
(25) Crank, J. *The Mathematics of Diffusion*; Oxford University Press: New York, 1957. See section 6.33.25.
(26) See Table 6.1 of ref 25.
(27) Morrison, M. E. Ph.D. Dissertation, The University of Texas at Austin, May 1997.
(28) This is also found in the independent experiments reported in ref 8.
(29) In this case $x_{buffer}(t) = (x_{buffer}(\infty) - x_{buffer}(0))(1 - e^{-kt}) + x_{buffer}(0)$.
(30) Clements, J. Research in progress.
(31) Kalyanasundaram, K.; Thomas, J. K. *J. Am. Chem. Soc.* **1997**, *99*, 22039.
(32) Dong, D. C.; Winnik, M. A. *Photochem. Photobiol.* **1982**, *35*, 17.
(33) $M(t)/M(\infty) = 1 - (6/\pi^2)\sum_{n=1}^{\infty}(1/n^2)\exp\{-Dn^2\pi t/R_s^2\}$, from ref 25, eq 6.20, where $M(t)$ corresponds to the total amount of probe inside the sphere.
(34) Of course pyrene and phenathrene are not what one would normally think of as good solvents. Undoubtedly very significant plasticization would be observed with species such as benzene.
(35) The amount of probe is very small. For example, for PS−PMA and pyrene, the total concentration of the probe after dilution is ca. 369×10^{-6} M/300 = 1.23×10^{-6} M, or 3.69 nmol in the 3 mL total volume.
(36) Berens, A. R.; Hopfenberg, H. B. *J. Membrane Sci.* **1982**, *10*, 283. These authors find the best exponential correlation when using the molecular diameters for molecules that are roughly spherical.
(37) Krevelen, D. W. *Properties of Polymers: Their Correlation with Chemical Structure: Their Numerical Estimation and Prediction from Additive Group Contributions*; Elsevier: Amsterdam, New York, 1990.
(38) Deppe, D. D.; Dhinojwala, A.; Torkelson, J. M. *Macromolecules* **1996**, *29*, 3898. In this paper one of the probes studied was pyrene in poly(isobutyl methacrylate) at temperatures from T_g (64 °C) to T_g + 20 °C, obtaining values from ca. 3×10^{-12} to 3×10^{-13} cm²/s.
(39) Bergbreiter, D. E.; Gray, H. N.; Srinivas, B. *Macromolecules* **1994**, *27*, 7294 and references to earlier work therein.
(40) A similar conclusion was reached for micelles with a fluorescence probe at the interface between the core and the corona (Eckert, A. R.; Martin, T. J.; Webber, S. E. *J. Phys. Chem.* **1997**, *101*, 1646).
(41) Shusharina, N. P.; Nyrkova, I. A.; Khokhlov, A. R. *Macromolecules* **1996**, *29*, 3167.
(42) In the earlier work, ref 7, the partition coefficient for phenanthrene in PS−PMA was determined from the kinetic fit to be ca. 4×10^5 and the diffusion constant was ca. 1×10^{-18} cm²/s. In the present study we obtain $K_P^0 = 0.95 \times 10^5$ from a direct determination and $D = 1 \times 10^{-17}$ cm²/s. The micelle loading procedure for the present studies was different from that for the earlier work, but it is not clear why this would affect the diffusion constant.

MA971721U